PFC/JA-82-14

Analysis of Toroidal Magnet Systems on the Basis of The Reissner Shell Theory

E.S. Bobrov, J. H. Schultz
Francis Bitter National Magnet Laboratory
Plasma Fusion Center
Massachusetts Institute of Technology,
Cambridge, MA 02139

THE AMERICAN SOCIETY OF MECHANICAL ENGINEERS
345 E. 47 St., New York, N.Y. 10017

82-PVP-32

ANALYSIS OF TOROIDAL MAGNET SYSTEMS ON THE BASIS OF THE REISSNER SHELL THEORY

E.S. Bobrov, J.H. Schultz
Francis Bitter National Magnet Laboratory
Plasma Fusion Center
Massachusetts Institute of Technology
Cambridge, Massachusetts 02139

ABSTRACT

A method for analyzing the structural behavior of toroidal magnet systems subjected to Lorentz forces both in and out of the winding planes, and thermal loads is considered in this paper. The toroidal coil assembly is treated as a finite thickness, orthotropic, rotationally symmetric shell of revolution acted upon by symmetrical and antisymmetrical loads. The equations based on Reissner's shell theory are derived, and numerical solutions are presented. The method is an efficient design tool for the analysis and shape selection of toroidal magnet systems and their structures, such as the in-plane and out-of-plane load support systems for closed magnetic confinement machines, e.g. tokamaks, stellarators, and bumpy tori.

NOMENCLATURE

B_t	toroidal magnetic field, T
B_v	vertical magnetic field, T
E_1, E_2, E_3	Young's moduli, N/m^2
F_z	vertical force, N
G_{12}, G_{13}, G_{23}	shear moduli, N/m^2
h	shell thickness, m
I	electric current, A
M_1, M_2, M_{12}, M_{21}	stress couples, Nm/m
N	number of toroidal turns
N_1, N_2, N_{12}, N_{21}	membrane stress resultants, N/m
Q_1, Q_2	transverse shear resultants, N/m
q_2, q_3	distributed shear and normal loads, N/m^2
r_1	toroidal radius, m
R_1, R_2	principal radii of curvature of middle surface, m
S	distance measured along the meridian, m
T, T_o, T_1	temperature increment and temperature resultants, °C
u,v,w	components of midsurface displacement, m
z	midsurface normal coordinate
α_1, α_2	coefficients of thermal expansion
β_1, β_2	angles of midsurface rotation
$\gamma_{12}, \gamma_{13}, \gamma_{23}$	shear strains
$\gamma_{13m}, \gamma_{23m}$	effective transverse shear strains
$\varepsilon_1, \varepsilon_2, \varepsilon_3$	axial strains
$\varepsilon_{1m}, \varepsilon_{2m}, \varepsilon_{12m}$	effective midsurface strains

Contributed by the Pressure Vessel & Piping Division of the ASME.

Θ	tangent of angle of meridian
$\kappa_1, \kappa_2, \kappa_{12}$	effective midsurface curvature changes
μ_o	magnetic permiability of vacuum, H/m
$\nu_{12}, \nu_{13}, \nu_{23}$	Poisson's ratios
$\sigma_1, \sigma_2, \sigma_3$	axial stresses
$\tau_{12}, \tau_{13}, \tau_{23}$	shear stresses
ϕ	equatorial coordinate
Ω	Lagrangean multiplier function

INTRODUCTION

This paper presents equations of orthotropic, rotationally symmetric toroidal shells of finite thickness subjected to symmetrical and antisymmetrical loads, including thermal loads. These equations were derived using the approach developed by E. Reissner (1) that allows to take into account the effect of transverse stresses on the deformation of the middle surface of the shell and consistently omit terms which are small of order h^2/R^2.

The equations are used to model the structural behavior of discrete and continuous toroidal field (TF) magnet systems subjected to in-plane and out-of-plane Lorentz forces and experiencing orthotropic thermal expansion or contraction.

The utilization of the theory of orthotropic shells of finite thickness for the structural analysis of the TF magnet systems is found to be very efficient, particularly in the process of initial shape selection.

The earliest and the most popular TF coil configuration, known as the Princeton D shape, was first derived in (2) by considering the equilibrium of a plane filament in pure tension subjected to a distributed normal load inversely proportional to the toroidal radius. The inner leg of this coil is supported by a stiff cylinder to react the unbalanced centering force. As shown by several authors (3-5) substantial bending stresses are revealed by detailed analyses of TF magnet structures designed to follow the pure tension trajectory. Large bending stresses were also found in the compound-constant-tension coil configurations derived in (6). These bending stresses were partially explained by several factors, including the finite thickness of the coils in real tokamak structures(7), nonuniformity of the toroidal field due to the discrete character of coil placement(8) and the violation of the compatibility conditions at the joining points of different "pure tension" shapes (9). Almost no consideration was given to the effect of the intercoil structure (to support the out-of-plane loads) on the coil shapes.

An important contribution in the modelling of toroidal magnet systems was the membrane shell model developed by Gray et al (10) which took into consideration the circumferential stiffness of the magnet assembly. A bending free membrane shell shape was derived. It was substantially different from that of a constant tension filament. Unlike the significant shape deviations described in (11) and (12), the deviation from the D trajectory happens in the membrane shell consideration naturally, independent of reaction forces or finite thickness effects. Unfortunately, there is an inherent strain incompatibility at the crown of a toroidal shell in the solution to the linear membrane theory (13). This incompatibility introduces bending stresses in a shell with finite bending stiffness, as demonstrated below.

This analysis and design studies (14) call into question the entire approach of searching for an optimal shape to minimize bending stresses. The analysis presented in this paper shows that typical tokamak reactor designs (14) with sufficient structural case material to withstand tensile stresses have sufficient bending stiffness to react the bending stresses, which were found to be less than 50% of primary membrane stresses, for the two shapes considered. Furthermore, design studies (14) of high-cycle, inductively driven tokamaks showed that case thicknesses were dominated by pulsed out-of-plane loads. The possibility of low-cycle operation for all the major toroidal confinement systems requires a capability for the rapid scoping of complex interrelated structural and physics trade-offs which is substantially advanced by the inclusion of the out-of-plane load induced stresses in the model described below.

BASIC EQUATIONS

Following E. Reissner(1) we derived a basic set of equations of rotationally symmetric orthotropic shells of revolution of finite thickness. The equations take into account the effect of transverse stresses on the deformation of the middle surface of the shell and retain terms of order h/R in comparison with unity. This is essential with an h/R ratio greater than 1/20. In order to distinguish the structural response of toroidal coil systems to symmetrical (normal pressure due to the toroidal field, and temperature variation) and antisymmetrical (torsional shear due to the vertical field) loads, the equations are presented in two respective groups of which the first corresponds to the symmetrical load and the second to the antysimmetrical load.

Symmetrical Load

In this case the shell is subjected to a mechanical pressure caused by toroidal field B_t

$$q_3 = \frac{\mu_o N^2 I^2}{8\pi^2 r^2}, \tag{1}$$

and rotationally symmetric temperature distribution $T(s,z)$. The temperature distribution in the shell is accounted for in the usual manner by means of the integrated temperature effect of the form

$$T_o(s) = \frac{1}{h}\int_{-\frac{h}{2}}^{\frac{h}{2}} T(s,z)dz \tag{2}$$

$$T_1(s) = \frac{12}{h^3}\int_{-\frac{h}{2}}^{\frac{h}{2}} zT(s,z)dz \tag{3}$$

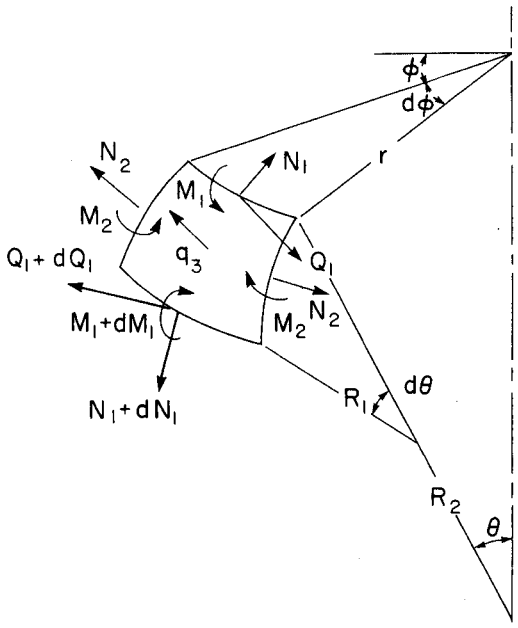

Fig. 1 Differential element of a shell of revolution under symmetric loading.

Equations of Equilibrium. Stress resultants and stress couples acting upon a differential element of the shell are in case of a symmetrical load as shown in Fig. 1. The equations of equilibrium in this case are

$$\frac{dN_1}{ds} + \frac{1}{r}\frac{dr}{ds}(N_1 - N_2) + \frac{Q_1}{R_1} = 0, \tag{4}$$

$$-\frac{N_1}{R_1} - \frac{N_2}{R_2} + \frac{dQ_1}{ds} + \frac{1}{r}\frac{dr}{ds}Q_1 = -q_3 \tag{5}$$

$$-Q_1 + \frac{dM_1}{ds} + \frac{1}{r}\frac{dr}{ds}(M_1 - M_2) = 0 \tag{6}$$

Stress-Strain and Strain-Displacement Relations. If the material of the shell is orthotropic, the following relations are true (15).

$$\varepsilon_1 = \frac{1}{E_1}(\sigma_1 - \nu_{21}\sigma_2 - \nu_{31}\sigma_3) \tag{7}$$

$$\varepsilon_2 = \frac{1}{E_2}(-\nu_{12}\sigma_1 + \sigma_2 - \nu_{32}\sigma_3) \tag{8}$$

$$\varepsilon_3 = \frac{1}{E_3}(-\nu_{13}\sigma_1 - \nu_{23}\sigma_2 + \sigma_3) \tag{9}$$

$$\gamma_{13} = \frac{1}{G_{13}}\tau_{13} \tag{10}$$

and

$$\frac{\nu_{12}}{E_2} = \frac{\nu_{21}}{E_1}, \quad \frac{\nu_{13}}{E_3} = \frac{\nu_{31}}{E_1}, \quad \frac{\nu_{23}}{E_3} = \frac{\nu_{32}}{E_2} \tag{11}$$

The stress-strain relations for the shell are obtained by minimizing the strain energy expressed in terms of stress resultants and stress couples, with equilibrium equations (4)-(6) as side conditions, using Lagrangean multipliers.

$$\varepsilon_{1m} = \alpha_1 T_o + \frac{N_1 - \nu_{21}N_2}{E_1 h} + \left(\frac{h}{R_1} - \frac{h}{R_2}\right)\frac{M_1}{E_1 h^2} + \frac{1}{E_3 h^2}\left[1.2\,\nu_{13}\frac{h}{R_1}M_1 + \left(\nu_{13}\frac{h}{R_2} + 0.2\,\nu_{23}\frac{h}{R_1}\right)M_2\right] \tag{12}$$

$$\varepsilon_{2m} = \alpha_2 T_o + \frac{N_2 - \nu_{12}N_1}{E_2 h} + \left(\frac{h}{R_2} - \frac{h}{R_1}\right)\frac{M_2}{E_2 h^2} + \frac{1}{E_3 h^2}\left[\left(0.2\,\nu_{13}\frac{h}{R_2} + \nu_{23}\frac{h}{R_1}\right)M_1 + 1.2\,\nu_{23}\frac{h}{R_2}M_2\right] \tag{13}$$

$$\gamma_{13m} = \frac{1.2}{G_{13} h}Q_1 \tag{14}$$

$$\kappa_1 = \alpha_1 T_1 + \frac{12(M_1 - \nu_{21}M_2)}{E_1 h^3} + \left(\frac{h}{R_1} - \frac{h}{R_2}\right)\frac{N_1}{E_1 h^2} + \frac{1}{E_3 h^2}\left[1.2\,\nu_{13}\frac{h}{R_1}N_1 + \left(0.2\,\nu_{13}\frac{h}{R_2} + \nu_{23}\frac{h}{R_1}\right)N_2\right] \tag{15}$$

$$\kappa_2 = \alpha_2 T_1 + \frac{12(M_2 - \nu_{12}M_1)}{E_2 h^3} + \left(\frac{h}{R_2} - \frac{h}{R_1}\right)\frac{N^2}{E_2 h^2} + \frac{1}{E_3 h^2}\left[\left(\nu_{13}\frac{h}{R_2} + 0.2\,\nu_{23}\frac{h}{R_1}\right)N_1 + 1.2\,\nu_{23}\frac{h}{R_2}N_2\right] \tag{16}$$

The effective midsurface strains and midsurface curvature changes are expressed in terms of the effective midsurface linear and angular displacements u, w, and β_1

$$\varepsilon_{1m} = \frac{du}{ds} + \frac{w}{R_1} \tag{17}$$

$$\varepsilon_{2m} = \frac{1}{r}\frac{dr}{ds}u + \frac{w}{R_2} \tag{18}$$

$$\gamma_{13m} = \beta_1 + \frac{dw}{ds} - \frac{u}{R_1} \tag{19}$$

$$\kappa_1 = \frac{d\beta_1}{ds} \tag{20}$$

$$\kappa_2 = \frac{1}{r}\frac{dr}{ds}\beta_1 \tag{21}$$

Antisymmetrical Load

In this case the load applied to the midsurface of the shell is the distributed shear

$$q_2 = \frac{B_v NI}{2\pi r}\cos\theta \tag{22}$$

which is antisymmetric with respect to the equatorial plane $\theta = \pm \pi/2$.

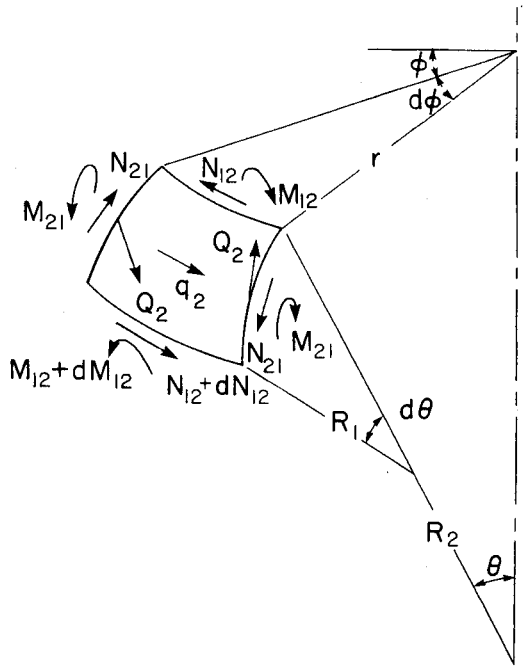

Fig. 2 Differential element of a shell of revolution under antisymmetric loading.

Equations of Equilibrium. In case of an antisymmetrical distributed shear load (22) only shear stress resultants and shear stress couples are generated in the shell as shown in Fig. 2. The equilibrium of the shell is described by the following four equations.

$$\frac{dN_{12}}{ds} + \frac{1}{r}\frac{dr}{ds}\left(N_{12} + N_{21}\right) + \frac{Q_2}{R_2} = -q_2 \tag{23}$$

$$\frac{dM_{12}}{ds} + \frac{1}{r}\frac{dr}{ds}\left(M_{12} + M_{21}\right) - Q_2 = 0 \tag{24}$$

$$N_{12} - N_{21} + \frac{M_{12}}{R_1} - \frac{M_{21}}{R_2} = 0 \tag{25}$$

$$M_{12} - M_{21} - \frac{h^2}{24}\left(\frac{1}{R_2} - \frac{1}{R_1}\right)\left(N_{12} + N_{21}\right) = 0 \tag{26}$$

Stress-Strain and Strain-Displacement Relations. The constitutive relationships (Hooke's law) if only shear strains and stresses are involved are expressed for an orthotropic material in the form

$$\gamma_{12} = \frac{1}{G_{12}}\tau_{12}, \quad \gamma_{23} = \frac{1}{G_{23}}\tau_{23} \tag{27}$$

Minimization of the shear strain energy expressed in terms of shear stress resultants N_{12}, N_{21}, Q_{23} and shear stress couples M_{12} and M_{21} yields three constitutive relationships

$$\varepsilon_{12m} = \frac{1}{4G_{12}h}\left(N_{12} + N_{21}\right) \tag{28}$$

$$\gamma_{23m} = \frac{1.2}{G_{23}h}Q_2 \tag{29}$$

$$\kappa_{12} = \frac{3}{G_{12}h^3}\left(M_{12} + M_{21}\right) \tag{30}$$

Utilization of the four equilibrium equations (23) - (26) by means of the Lagrange multiplier method leads to expressions for the effective midsurface shear strain and curvature variations in terms of the effective midsurface linear displacement v and angular displacement β_2.

$$\varepsilon_{12m} = \frac{1}{2}\left(\frac{dv}{ds} - \frac{1}{r}\frac{dr}{ds}v\right) + \frac{h^2}{24}\left(\frac{1}{R_1} - \frac{1}{R_2}\right)\Omega \tag{31}$$

$$\Omega = -\frac{1}{4}\left(\frac{1}{R_1} + \frac{1}{R_2}\right)\left(\frac{dv}{ds} + \frac{1}{4}\frac{dr}{ds}v\right) + \frac{1}{2}\left(\frac{d\beta_2}{ds} + \frac{1}{r}\frac{dr}{ds}\beta_2\right) \tag{32}$$

$$\kappa_{12} = \frac{1}{2}\left(\frac{d\beta_2}{ds} - \frac{1}{r}\frac{dr}{ds}\beta_2\right) + \frac{1}{4}\left(\frac{1}{R_2} - \frac{1}{R_1}\right)\left(\frac{dv}{ds} + \frac{1}{r}\frac{dr}{ds}v\right) \tag{33}$$

$$\gamma_{23m} = \beta_2 - \frac{v}{R_2} \tag{34}$$

NUMERICAL IMPLEMENTATION AND RESULTS

The solutions to the equations presented above, with appropriate boundary conditions give a complete description of the behavior of an orthotropic shell of revolution, of finite thickness.

In order to obtain the necessary quantities

$$\frac{1}{R_1}, \quad \frac{1}{R_2}, \text{ and } \frac{1}{r}\frac{dr}{ds},$$

which enter as coefficients into equations, the meridian of the shell should be described as a function of s or r, either analytically or in a tabulated form

The geometrical identities used to describe the shell of revolution are:

$$\frac{dr}{ds} = \cos\theta \tag{35}$$

$$\frac{1}{R_1} = \frac{d(\sin\theta)}{dr} \tag{36}$$

$$\frac{1}{R_2} = \frac{\sin\theta}{r} \tag{37}$$

A computer code for the finite difference solution of the two groups of equations corresponding to symmetrical and antisymmetrical loadings has been developed. In order to complete the analysis, the code requires the analytical or tabulated expression for the shape of the meridian in the form

$$\sin\theta = f(r) \tag{38}$$

along with the inner and outer toroidal radii, effective material physical properties, and the number of ampere-turns.

The meridian shapes presented here as examples are a circle and the "bending free" shell of Gray et al (10). Both shells have dimensions of the toroidal field coils in the Fusion Engineering Device (FED) described in (14), i.e., r_{in} = 2.14 m, r_{out} = 10.5 m, NI = 115 MAT, effective shell thickness h = 0.66 m and a coil case thickness 0.08 m. Figure 3 shows the meridians of the circular and "bending free" shells analyzed in this paper, along with that of a Princeton D.

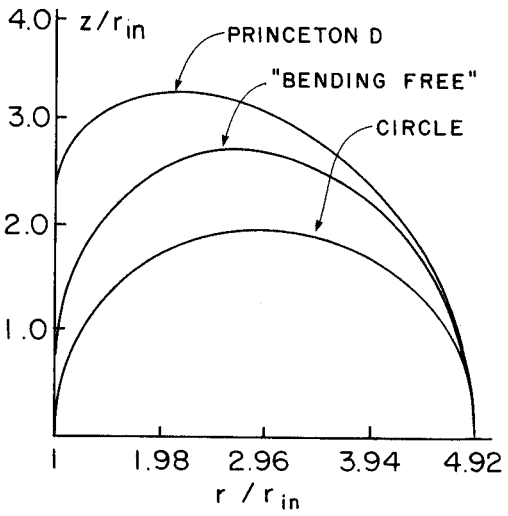

Fig. 3 Meridians of circular, "bending free", and Princeton D tori for FED aspect ratio.

The results of the analyses are presented in Fig. 4 and Fig. 5. Figure 4 shows the distribution of the effective meridional and circumferential membrane stresses in the coils and intercoil structures of both shapes. The effective meridional and circumferential bending stresses in the extreme fibers of the structural elements are as shown in Fig. 5. For the circular configuration the primary tensile stress at the inner leg at the equator is 151 MPa while the peak bending stress is 54 MPa. For the "bending free" configuration, the primary tensile stress in the inner leg at the equator is 139 MPa, while the peak bending stress is 66 MPa.

This demonstrates that if the finite thickness of the magnet structure is accounted for the "bending free" configuration proposed in (10) has bending stresses which are proportionally as large as the bending stresses in the circular configuration.

Since the total upward force on the upper half of the coil system must be

$$F_z = \frac{\mu_o (NI)^2}{4\pi} \ln \frac{r_{out}}{r_{in}} \qquad (39)$$

or 2122 MN, the theoretical minimum tension is 1061 MN in the inner leg, giving an average stress of 120 MPa in an ideal constant tension coil. Thus, the tensile stress in the inner leg at the equator for

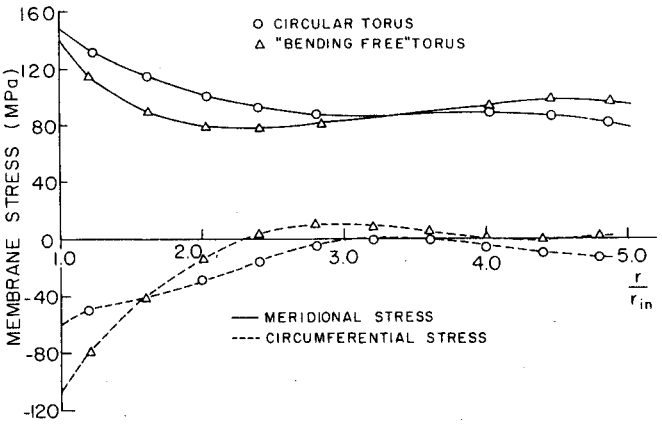

Fig. 4 Effective membrane stresses in circular and "bending free" coil structures with FED dimensions.

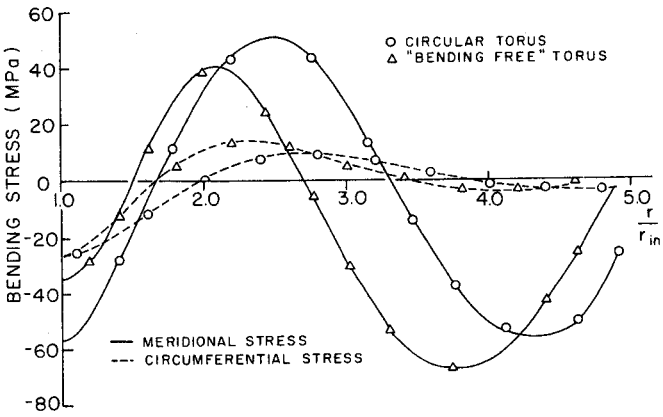

Fig. 5 Effective bending stresses in the extreme fibers of circular and "bending free" coil structures with FED dimensions.

circular coil is 1.26 times the theoretical minimum, while the tensile stress for the "bending free" configuration is 1.16 times the theoretical minimum. The primary stress in the "bending free" shape is 8.5% smaller than that in the circle, while the perimeter of the "bending free" configuration is 18% greater than that of a circle, implying that the circular configuration requires less mass for a given set of stress allowables.

CONCLUSIONS

An efficient method of analysis of toroidal magnet structures of arbitrary configuration, and subjected to electromechanical and thermal loads has been developed and numerically implemented.

It has been found that due to the finite thickness of realistic magnet structures and discontinuity of the displacement field present in the linear membrane theory the "bending free" shell configuration derived in (10) has bending stresses.

The whole concept of shape optimization based on minimization of bending stresses is called into

question. The design strategy of simply making the toroidal field coils circular or as small as possible, within the constraints of reactor assembly and maintenance can be recommended as an alternative. Reactor concepts with all external vertical field coils could be substantially reduced in weight and cost by using low profile coils.

ACKNOWLEDGMENTS

This work was supported by the Office of Fusion Energy, U.S. Department of Energy, under contract DOE/ET-51013-31. The Francis Bitter National Magnet Laboratory receives support from the National Science Foundation.

REFERENCES

1 Reissner, E., "On Some Problems in Shell Theory," Structural Mechanics, Proceedings of the First Symposium on Naval Structural Mechanics, Pergamon Press, New York, 1960, pp. 74-113.

2 File, J., Mills, R.G., and Sheffield, G.V., "Large Superconducting Magnet Designs for Fusion Reactors," IEEE Transactions of Nuclear Science, NS-18, 1971, pp. 277-282.

3 DeMichele, D.W., Darby, J.B., Jr., "Three-Dimensional Mechanical Stresses in Toroidal Magnets for Controlled Thermonuclear Reactors," Proceedings of the Fifth Symposium on Engineering Problems of Fusion Research, 1974, pp. 558-569.

4 Söll, M., "Comparison of Some Analytical and Numerical Calculated Parameters for Toroidal Field Coils," IPP 4/145, Nov. 1976, Max-Plank Institute for Plasma Physics, Munich, Federal Republic of Germany.

5 Diserans, N.J., "Stress Analysis Studies in Optimized 'D' Shaped Tokamak Magnet Designs," RL-75-117, July 1975, Rutherford Laboratory, Chilton, Didcot, Oxon, England.

6 Gralnick, S.L., and Tenney, F.H., "Analytic Solutions for Constant Tension Coil Shapes," Journal of Applied Physics, Vol. 47, No. 6, June 1976, pp. 2710-2715.

7 Weissenburger, D.W., Christensen, U.R., Bialek, J., "Pure Tension Shape of a Thick Torus," PPPL-1353, July 1977, Princeton Plasma Physics Laboratory, Princeton, N.J.

8 Moses, R.W., and Young, W.C., "Analytical Expressions for Magnetic Forces on Sectored Toroidal Coils," Proceedings of the Sixth Symposium on Engineering Problems of Fusion Research, 1976, pp. 917-921.

9 Gralnick, S.L., Ojalvo, I.U., Zatz, I.J., and Balderes, T., Nuclear Technology, Vol. 45, No. 10, October 1979, pp. 233-243.

10 Gray, W.H., Stoddart, W.C.T., Akin, J.E., "A Derivation of a Bending Free Todoidal Shell for Tokamak Fusion Reactors,"Journal of Applied Mechanics, Vol. 46, March 1979, pp. 120-124.

11 Welch, C.T., "Bending-Free Shapes for Toroidal Magnet Field Coils with Concentrated Symmetric Reactions," Proceedings of the Sixth Symposium on Engineering Problems of Fusion Research, 1976, pp. 410-913.

12 Ojalvo, I.U., and Zatz, I.J., "Structural Support Design Method for Minimizing In-Plane TF Coil Stresses," Proceedings of the Eighth Symposium on Engineering Problems of Fusion Research, 1980, pp. 1463-1468.

13 Flügge, W., Stresses in Shells, 2nd Ed., Springer-Verlag, Berlin, 1973.

14 Flanagan, C.A., Steiner, D., Smith, G.E., Fusion Engineering Design Center Staff, "Fusion Engineering Design Description," Vol. 1, ORNL/TM-7948/V1, December 1981, Oak Ridge National Laboratory, Oak Ridge, Tennessee.

15 Lekhnitski, S.G., Theory of Elasticity of Anisotropic Elastic Body, Holden-Day, San Francisco, California, 1963.